ISBN: 978-3-95450-184-7 doi:10.18429/JACoW-IPAC2018-THPAL061

SIMULATION OF PULSED TEMPERATURE RISE IN CRYOGENIC COPPER RF CAVITY ACHIEVING A VERY HIGH ACCELERATING FIELD

T. Tanaka†, K. Hayakawa, Y. Hayakawa, K. Nogami, T. Sakai, Y. Sumitomo
Laboratory for Electron Beam Research and Application, Nihon University, Funabashi, Japan

Abstract

On the basis of the cold model of a cryogenic C-band copper photocathode rf gun cavity, characterized by a low wall loss and high Q factor at 20 K, the temperature rise at the wall surface of the cavity during the rf pulse has been simulated with the one-dimensional thermal diffusion model. The simulation with rough approximations has shown that the temperature at the side wall surface rises by approximately 44 K at the end of the 50 MW rf pulse duration of 2 µs. On the other hand, the accelerating gradient estimated simultaneously has shown an enhancement up to 340 MV/m, which is due to the increase in the rf transmission into the cavity caused by the temperature rise. The increasing field during the rf pulse is not desirable for the investigation of vacuum breakdown phenomena at very high electric fields. Simulations of the input rf power modulation for the cavity with a smaller coupling coefficient has suggested that the modulation is effective to keep a constant accelerating gradient for over 1.2 µs even at a gradient as high as 363 MV/m.

INTRODUCTION

Recent studies on the vacuum rf breakdown at high electric fields suggest that the temperature in the cavity surface during the high power rf pulse has a significant effect on the behaviour of the breakdown rate [1, 2]. This also suggests that a cryogenic copper rf cavity operated at temperatures as low as 20 K is a candidate for a structure achieving an accelerating gradient of multiple 100 MV/m.

The properties of a cryogenic C-band photocathode rf electron gun cavity were studied at the Laboratory for Electron Beam Research and Application (LEBRA) in Nihon University as a collaboration with KEK [3]. The cryogenic properties of the cold model cavity fabricated in the collaboration were measured later at LEBRA, which have shown good agreement with those expected from computer simulations using the surface resistance of the copper cavity predicted by the theory of the anomalous skin effect [4]. High power tests with a newly designed cryogenic cavity ares under consideration for the study of vacuum breakdown phenomena at very high electric fields.

This paper reports the simulations of the behaviours of the temperature rise and the accelerating gradient in the high power rf pulse duration on the previous model and the cavity with a smaller coupling coefficient.

PULSE HEATING OF CAVITY SURFACE

Figure 1 shows the magnetic field distribution in the cold model cavity at 20K obtained by the CST Studio simulation. In the following discussions we assume that the input

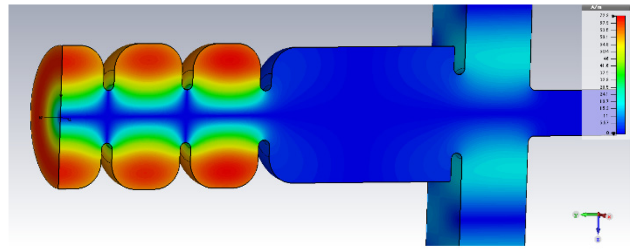

Figure 1: Magnetic field distribution in the cold model cavity by the CST Studio simulation [5].

Table 1: Specifications and the Power Dissipated in the Cryogenic 2.6-cell RF Gun Cavity at 20 K

$TM_{01\pi}$ frequency	5712	MHz
RRR of 6N8 high purity copper	> 3000	
Unloaded Q	73000	
Coupling coefficient	19.7	
Peak input rf power	4	MW
Peak power dissipation	0.736	MW
Pulse duration	2	µs
Surface resistance	3.65	mΩ
Maximum surface electric field	162	MV/m
Accelerating gradient	83.0	MV/m
Average peak surface loss	5.15	kW/cm^2
Maximum peak surface loss	7.20	kW/cm^2
Side wall peak surface loss	5.83	kW/cm^2

rf power is dissipated only in the accelerating cells, since the losses in the coupler and the mode converter are small compared to that in the accelerating cells. Table 1 lists the specifications and the rf power dissipated at the surface of the cavity for the input power of 4 MW, where the temperature rise is not taken into account. Due to the large coupling coefficient, $\beta = 19.7$, the total power dissipated in the cavity is 0.736 MW. The dissipation per unit surface area, dP/dS, at each point of the surface is given by the amplitude of the surface magnetic field H and the surface resistance R_S at that point as

$$\frac{dP}{dS} = \frac{1}{2} R_S |H|^2 . \quad (1)$$

The average power dissipated per unit surface area was estimated from the total surface area over the 2.6 accelerating cells. The CST Studio simulation [5] has shown that the maximum dP/dS at the 0.6-cell end plate is 40 % higher than the average value. On the other hand, the dP/dS at the

† tanaka@lebra.nihon-u.ac.jp

ISBN: 978-3-95450-184-7 doi:10.18429/JACoW-IPAC2018-THPAL061

curved side wall surface is 13 % higher than the average value.

Since the wall loss at the cavity surface depends on R_S, the cavity properties drastically change as the surface temperature rises to 30 K or higher in contrast to room temperature operations. Therefore, the incoming and the outgoing electric fields at the input port of the cavity are obtained by solving the equation

$$\frac{dE_O(t)}{dt} = -\frac{\{1+\beta(t)\}\omega_0}{2Q_0(t)} E_O(t) + \frac{\beta(t)\omega_0}{Q_0(t)} E_I(t), \quad (2)$$

where E_I is the incoming field, E_O the outgoing field, Q_0 the unloaded quality factor, $\beta(t)$ the coupling coefficient which is also a function of the resonant frequency and the input rf frequency, ω_0, and t the time from the beginning of the rf pulse.

According to the one-dimensional thermal diffusion model [6], the temperature rise ΔT at the cavity wall surface that was caused by the pulse heating due to the rf power dissipation is expressed as

$$\Delta T(t) = \int_0^t \frac{1}{\sqrt{\pi\rho K(T) C_P(T)}} \frac{dP(t',T)}{dS} \frac{dt'}{\sqrt{t-t'}}, \quad (3)$$

where ρ is the mass density, K the thermal conductance, C_P the specific heat, T the temperature of the surface at the time t'. The product $K \times C_P$ is weakly dependent on the temperature in the region considered [7, 8]. After partial integral of Eq. (3), the numerical calculation can be simplified by ignoring the change in the product during each time step as

$$\Delta T(t) = \sum_{i=0}^{i=\frac{t}{\Delta t'}-1} \frac{2\sqrt{t-t'_i}}{\sqrt{\pi\rho K(T_i) C_P(T_i)}} \frac{d}{dt'_i}\left\{\frac{dP(t'_i,T_i)}{dS}\right\}\Delta t'. \quad (4)$$

The ratio of the dP/dS, averaged over the accelerating 2.6 cell surface, and the total cavity loss is assumed to be the same as the case in Table 1. Thus the average dP/dS is deduced at each time step from the rf power dissipated in the cavity that was obtained by solving Eq. (2). Using the cavity surface temperature obtained by Eq. (4), $R_S(t)$, $Q_0(t)$, $\beta(t)$ and $\omega(t)$ are updated for the use in the next time step. Therefore, the simulation gives the average temperature rise and its effect on the properties of the cavity relative to the values in Table 1.

TEMPERATURE RISE IN THE COLD MODEL CAVITY

The cold model cavity was originally designed for the development of an rf gun cavity that operates with an input rf power of 4 MW at 20 K. However, the low loss and high efficiency property of the cavity obtained by cryogenic measurements is desirable to study vacuum breakdown

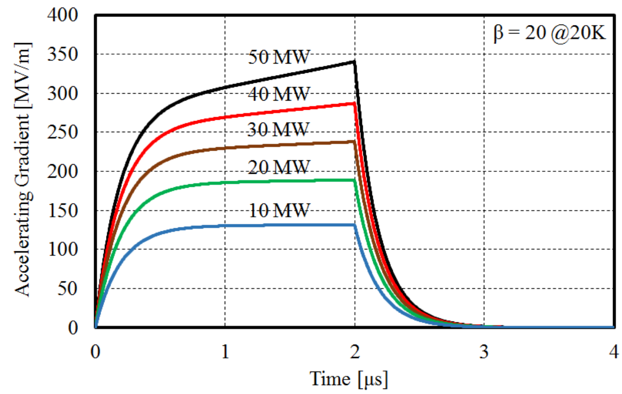

Figure 2: The accelerating gradient obtained with the cold model cavity for each input power.

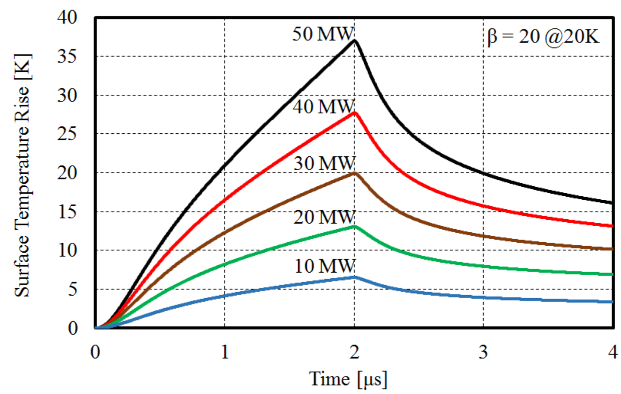

Figure 3: Average surface temperature rise in the cold model cavity for each input power.

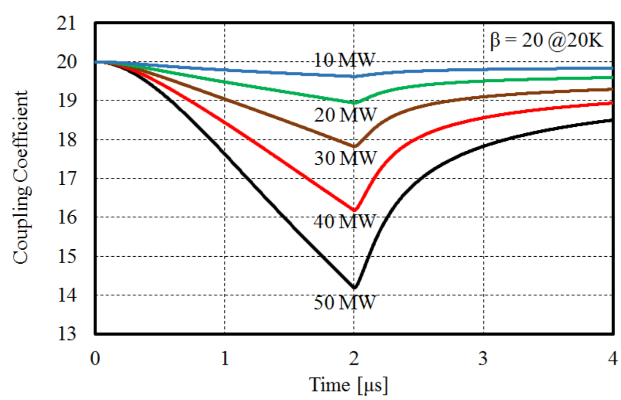

Figure 4: Decrease in the coupling coefficient due to the surface temperature rise.

phenomena under a high power and high electric field condition.

Figure 2 shows the accelerating gradient obtained by the simulations with the input of square rf pulses varied from 10 to 50 MW peak in 10 MW steps. The coupling coefficient β was assumed to be 20 at 20 K. The pulse duration is 2 μs. Figure 3 shows the average surface temperature rise corresponding to each input power. The highest accelerating gradient of 340 MV/m at the end of the input rf pulse of 50 MW peak, where the surface temperature rise is approximately 37 K, is 50 MV/m higher than the simu-

ISBN: 978-3-95450-184-7 doi:10.18429/JACoW-IPAC2018-THPAL061

lation result with no temperature rise. The maximum surface field of 660 MV/m at 50 MW of input is located near the edge of the curved disk aperture. From Fig. 2 it is clear that an enhancement of the accelerating gradient toward the end of the pulse is more significant at higher input powers. This is due to the positive feedback between the increasing temperature and the decreasing coupling coefficient followed by the increase in the transmitted power into the cavity. The change in the coupling coefficient is shown in Fig. 4, which is the result of the deterioration of Q_0 due to the increased surface resistance.

FIELD FLATTENING BY RF POWER MODULATION

The enhancement of the accelerating gradient as well as the maximum surface field during the rf pulse can be suppressed by modulating the input rf power. For simplicity in the simulation based on Eqs. (2) and (4), this actually has been made by introducing a modulating function $f(t)$ to the incoming electric field E_I as

$$E_I(t) = f(t)\,E_{I0}, \tag{5}$$

$$f(t) = \begin{cases} 1 & (t < t_s) \\ 1 - a\{1 + b(t - t_s)\}\{1 - \exp(-t/\tau_d)\} & (t \geq t_s) \end{cases}, \tag{6}$$

where E_{I0} is kept constant during the pulse, t_s the time the modulation begins, τ_d the time constant of the transition from the constant field amplitude, a and b the optimization parameters to flatten the field during the pulse.

In the simulations involving the rf power modulation, the basic configurations of the cavity were assumed to be the same as those at the cold model. The values $t_s = 0.75$ µs and $\tau_d = 10$ ns were used in common. With this condition the coupling coefficient was chosen to be 10 at 20 K in order to achieve a flat electric field higher than the maximum field reached at 50 MW of input shown in Fig. 2.

The results of the input rf power, the accelerating gradient, and the average surface temperature rise are shown in Fig. 5, Fig. 6 and Fig. 7, respectively. The parameters a and b were optimized to have a flatness within ± 0.1 % of the

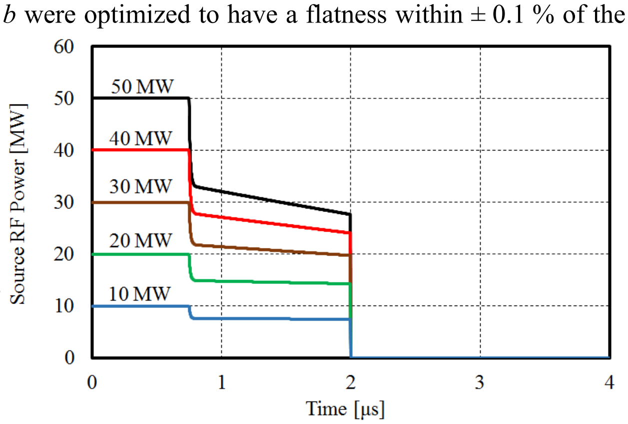

Figure 5: The waveforms of the input rf power modulated by the function in Eq. (6). The parameters a and b were optimized for each input rf power.

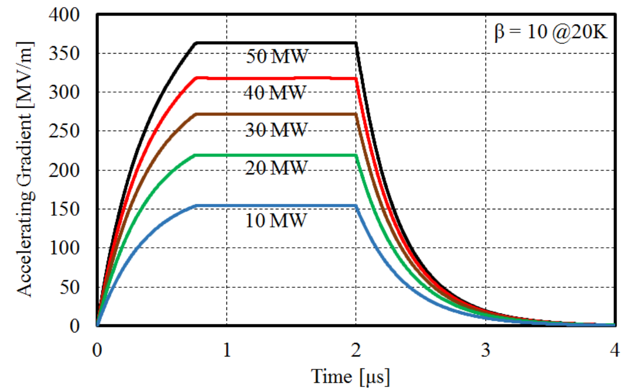

Figure 6: The flat accelerating gradient obtained with the input rf power modulation for each input power.

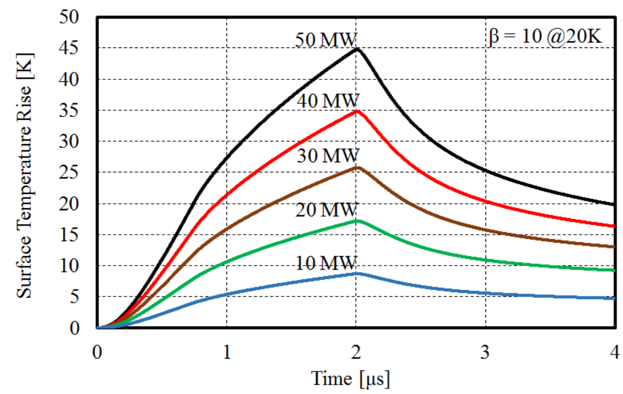

Figure 7: Average surface temperature rise when each input rf power was modulated as shown in Fig. 5.

fluctuation over 1.2 µs in each simulation. The accelerating gradient of 363 MV/m is achieved at 50 MW, while the maximum surface field is 709 MV/m at the curved disk region. The maximum temperature rise at 50 MW is approximately 8 K higher than that at the cold model cavity.

CONCLUSION

The simulations of the cavity surface temperature rise at the 2.6-cell cryogenic C-band rf gun cavity have suggested that the accelerating gradient of 340 MV/m is obtained with the peak input rf power of 50 MW. Simulations involving an input rf power modulation for the cavity with a coupling coefficient $\beta = 10$ could improve the field flatness to within the errors of ± 0.1 % over 1.2 µs. In this case, the study of the vacuum rf breakdown is possible at very high surface electric fields higher than 700 MV/m by using a 50 MW klystron.

REFERENCES

[1] K. Nordlund and F. Djurabekova, "Defect model for the dependence of breakdown rate on external electric fields", *Phys. Rev. ST Accel. Beams,* vol. 15, p. 071002, 2012.

[2] V. Dolgashev, "High gradient, X-band and above, metallic RF structures", presented at 2nd European Advanced Accelerator Concepts Workshop (EAAC 2015) (13-19 September, La Biodola, Isola d'Elba, Italy, 2015).

ISBN: 978-3-95450-184-7 doi:10.18429/JACoW-IPAC2018-THPAL061

[3] T. Tanaka *et al.*, "Characterization of cold model cavity of cryocooled C-band 2.6-cell rf gun at 20 K", *IOP Conf. Series: Journal of Physics: Conf. Series,* vol. 874, p. 012026, 2017.

[4] G. E. H. Reuter and E. H. Sondheimer, "The theory of the anomalous skin effect in metals", *Proc. the Royal Soc. of London* A, *Mathematical and Physical Sciences*, vol. 195, pp. 336-364, 1948.

[5] CST Studio Suite™, CST AG, Germany, http://www.cst.com

[6] D. P. Pritzkau, "Experimental study of rf pulsed heating on oxygen free electronic copper", *Phys. Rev. ST Accel. Beams*, vol. 5, p. 112002, 2002.

[7] J. G. Hust and A. B. Lankford, "Thermal conductivity of aluminum, copper, iron, and tungsten for temperatures from 1 K to the melting point", National Bureau of Standards, U.S. Department of Commerce, Boulder, CO, U.S.A.

[8] https://trc.nist.gov/cryogenics/materials/OFHC%20Copper/OFHC_Copper_rev1.htm